

FINITE ELEMENT MODELING OF GUARDRAIL TIMBER POSTS AND THE POST-SOIL INTERACTION

C A Plaxico¹, G S Patzner² and M H Ray³

Abstract - The performance of many guardrail terminal systems is dependent upon the strength of timber guardrail posts and soil conditions. Accurately simulating the breakaway characteristics of guardrail posts mounted in soils is an important issue concerning researchers in the roadside safety community. Finite element analysis is one method that can be used to evaluate roadside hardware designs, but good simulations are contingent upon developing accurate models of the components. This paper describes the development of a model of a breakaway timber post and soil system used in the Breakaway Cable Terminal (BCT) and the Modified Eccentric Loader BCT (MELT). The model is described and simulation results are compared to data from physical tests of BCT/MELT posts.

INTRODUCTION

Developing safer roadside hardware with more consistent performance is the objective of roadside safety hardware developers. Roadside safety hardware is designed to absorb large amounts of energy and safely redirect or stop errant vehicles. The analysis of such systems involves dynamic loading, large deformations, material failure and nonlinear material behavior and is much too complicated for standard linear-elastic analytical methods and closed form solutions. There are, however, two established methods which are often utilized to determine the crashworthiness of roadside hardware: 1) full-scale crash testing and 2) nonlinear explicit finite element simulation. The traditional and most widely accepted method over the past 30 years

-
1. Research Engineer, Center for Computer Aided Design, University of Iowa, Iowa City, IA 52242. 319-335-3379. cplaxico@ccad.uiowa.edu.
 2. Graduate Research Assistant, Center for Computer Aided Design, University of Iowa, Iowa City, IA 52242. gpatzner@ccad.uiowa.edu.
 3. Assistant Professor of Civil Engineering, Center for Computer Aided Design, University of Iowa, Iowa City, IA 52242. 319-384-0523. mhray@icaen.uiowa.edu.

has been full-scale crash testing. Nonetheless, the cost associated with crash tests is extensive and the analyst does not have complete control of the test conditions.

Since the early 1990's finite element analysis has rapidly become a fundamental part of the analysis and design of roadside safety hardware systems. In addition to being a reliable and relatively inexpensive means of analyzing and simulating impact events, it allows the analyst more control over the impact conditions and provides detailed information about the mechanics of the impact event.

Obtaining accurate simulations is dependent upon developing accurate models of each of the distinct components of the guardrail system and properly modeling their interaction with each other. Geometrical modeling of the constituents is becoming a relatively easy task due to the advancements in preprocessor technology, however, accurately characterizing material behavior is often a very challenging facet of finite element modeling. Simulating the material and physical behavior of wooden guardrail posts and the post-soil interaction of the soil mounted posts has been a principal concern to researchers developing finite element models of guardrail systems. Wood is an anisotropic fibrous material which exhibits a complex mode of failure in bending, due primarily to the difference in tensile and compressive strength of wood. Modeling the behavior of wood would be difficult with the existing anisotropic material models available in LS-DYNA3D due to limitations in the models' failure criteria. Furthermore, an extensive physical testing program would be required to determine the physical parameters of the model, which was beyond the scope of this research. There is, however, a simple isotropic material model available in LS-DYNA3D that is capable of accurately simulating the response and fracture of wood posts in bending and was therefore used in this study.

Though explicitly modeling the post embedded in a continuum of soil would be the most formidable method of modeling the post-soil interaction, it would not be the most practical due the immense computation required for the analysis of such a large model. Hence, alternative modeling techniques must be implemented to simulate the physical behavior of soil-mounted wood posts. In previous work the post-soil interaction has

been modeled such that the post was fixed at a point below grade rather than explicitly modeling the soil continuum and the post-soil interface.(1) Crash tests and finite element simulations have demonstrated, however, that the post-soil interaction can have considerable influence on the response of guardrail systems during vehicular impact.(2)(3)(4)(5) An alternative method of modeling the critical interaction between the soil and posts can be achieved by using the subgrade reaction approach in which an array of springs is attached from the post to the ground. The subgrade reaction method was utilized in this study to model the post-soil interaction.

TIMBER POSTS

Timber Material Properties

While metal materials are relatively easy to characterize and model using the standard material models in LS-DYNA3D, timber materials are much more challenging. LS-DYNA3D does not have a material model that is directly applicable to modeling the behavior of wood. Wood is a very complex anisotropic material that is often assumed to be orthotropic with its three principal material directions coinciding with the longitudinal, radial, and tangential directions of the wood grains. LS-DYNA3D has several composite material models that may be useful for modeling the orthotropic nature of wood, but the composite material models that may be used with brick elements do not allow for failure of the elements; a critical feature necessary for modeling breakaway timber posts.

Another disadvantage of using the composite material models for modeling wood is the lack of knowledge about wood properties. Although wood is often assumed to be an orthotropic material, there is very little and often contradictory information available pertaining to the associated material properties. The USDA Wood Handbook lists moduli of rupture, which is an upper bound measure of the ultimate strength of wood in bending, for green Douglas Firs and Southern Yellow Pines ranging from 45 MPa to 60 MPa.(6) The variability of wood properties in the literature is attributable to the fact that the properties of wood are

affected by many factors, such as, moisture content, density, material age and knots.

Fortunately, there are numerous ballistic pendulum tests of both standard 190x150 mm wood guardrail posts and the Breakaway Cable Terminal (BCT) posts available in the roadside hardware testing literature.(7) The observed ultimate stresses calculated from the pendulum tests agree reasonably well with the values listed in the Wood Handbook. Realistic material properties can be obtained through simulation of these pendulum tests.

The most formidable method of modeling the posts is to use a failing material model in LS-DYNA3D. The advantage to this approach is that the analyst need not know *a priori* where the failure is going to occur. Unfortunately, most of these material models are isotropic and better suited to metals than wood. Until a material model is developed that encompasses the complexity of an orthotropic material with failure and an extensive testing program is conducted to determine the physical parameters of such a model, the following simplified isotropic material model may be used.

The isotropic-elastic-plastic with failure material model (material type 13) in LS-DYNA3D does possess a desired feature for modeling the failure region of timber post. Its failure criteria enables an element to lose its ability to carry tension. When the effective plastic strain of an element reaches the failure strain or when the pressure reaches the tensile failure pressure, the deviatoric stresses are set to zero.(8)(9) The failure mode observed in wooden posts, in which the longitudinal fibers of the post progressively fail in tension due to bending on the impact face of the post, can be adequately simulated with this material model.

Finite Element Model

The timber post is modeled in LS-DYNA3D with eight-node solid hexahedron (brick) elements. The volume integration is carried out using one-point Gauss quadrature, except in the failure region of the post where a fourteen-point integration rule was employed. One-point integration is the default offered by the LS-DYNA3D code and it provides substantial savings in computation time over the eight-point, the fourteen-

point and the twenty-seven-point integrated elements, however, care should be taken to control the zero energy deformation modes (hourglassing) of the underintegrated solid elements. Even if the stiffness matrix is integrated by a 2 by 2 by 2 Gauss quadrature rule (eight-point integration) there is still the possibility of three zero energy modes, one involving each of the three orthogonal directions.⁽¹⁰⁾ One solution to the problem of “hourglassing” is to use the 3 by 3 by 3 Gauss quadrature rule (twenty-seven-point integration) which is very computationally demanding. An alternative solution is to use the special stabilization device offered in LS-DYNA3D which is a special fourteen-point rule that has nearly the same accuracy as the twenty-seven-point Gauss rule. Although there are substantial savings in computation cost by using the underintegrated elements, the fourteen-point integration rule is recommended to eliminate the zero energy modes.⁽⁸⁾

The finite element model of the post consists of a large number of solid elements. Consequently, modeling the posts using the fourteen-point integration elements and implementing it into large scale simulations, where many posts may be needed in the finite element model, may result in very large computation time. An alternative method to control the hourglassing modes of the underintegrated elements is to use the Flanagan-Belyschko stiffness form of hourglass control which has exact volume integration for solid elements.⁽⁹⁾ The one-point integration elements were used in the lower stress regions of the post model to reduce computation costs.

The failure mode of the breakaway timber posts, however, necessitated the use of the fourteen-point integration elements in the higher stress regions. The one-point integration rule was not applicable in the failure region because a single brick element in bending cannot develop the failure stress. An element using the one-point integration rule only calculates stresses at one point in the center of the volume, which would coincide with neutral axis of the bending moment in the element. With stresses only being calculated near the neutral axis of the element in bending, failure stress magnitudes cannot be reached. In early simulations of the failure of timber breakaway posts, the last row of elements on the failure plane would not fail for this

reason. Table 1 shows the properties of the two material models used in the wood posts.

Pendulum Test Comparison

In order to use the isotropic-elastic-plastic with failure material model, it was necessary to validate the failure mode against physical component tests. A series of pendulum tests of wooden BCT posts was conducted at the Federal Outdoor Impact Laboratory (FOIL) for this purpose.⁽⁷⁾ The tests were conducted on five standard BCT posts to measure the force and impulse required to break the post.

The vehicle used in the pendulum tests was an 839-kg pendulum with a crushable nose. The pendulum consisted of a reinforced concrete mass suspended from a steel structure by four steel cables. Within the concrete mass were two aluminum guide tubes; a sliding nose was inserted into the guide tubes; and multiple cartridges of an expandable aluminum honeycomb material were placed inside the sliding nose to simulate actual vehicle crush. The honeycomb was configured to simulate a 1979 Volkswagon Rabbit's left quarter point.

A model of the crushable nose pendulum was developed at the National Crash Analysis Center (NCAC). The crushable nose vehicle model was modeled as a steel frame cart with the crushable nose rather than modeling the pendulum suspended by steel cables. The overall impact responses between the pendulum and the bogie model were very similar and the model was validated with comparisons to the pendulum test data. One minor change was made to the honeycomb properties in the bogie vehicle obtained from the NCAC so that the properties would coincided with the ones used in the physical tests; the third stage of the honeycomb was made to have the same static crush strength as the first stage.

Figure 1 shows the test and simulation configuration. The pendulum impacted the posts at approximately 32 km/h. The centerline of the crushable nose was aligned with the center of the wood posts. In the tests, the posts were mounted in steel foundation tubes bolted to rigid concrete footings. This allowed for the wood properties to be isolated in the physical tests. In simulation, this boundary condition was

modeled using a steel foundation tube and soil plate concept resembling the mounting conditions used for guardrail terminal post installation. Any difference in ground-line deflection between either of these mounting conditions is very minimal.

The foundation tube (PTE05) and soil plate (PLS03) were not modeled physically. Instead, an extension of the BCT post to coincide with the length of a foundation tube was modeled. The yield stress of the steel foundation tube was used for this extension. Also, the density of this extension was calculated as a composite density of the wood and foundation tube. The mounting conditions were set by using the soil model described in the next section of this paper. In addition to using a strong soil, the width of the soil plate was used for calculating the load curves that define the stiffness of the soil along region of the post model where the soil plate appears physically. The larger the width used in load curve calculations, the higher is the resisting force of the soil. An extremely strong soil model was used in the simulation of the pendulum tests to correspond to the fixed mounting conditions used in the test.

A comparison between the tests and simulation were made by using the properties listed in Table 1, with the only varying parameter being the failure pressure of the material in the failing region around the breakaway hole. Figure 2 shows the acceleration curves of the five standard BCT post pendulum tests. Three of the tests had very similar responses (bold), while two showed somewhat stronger responses. Test 91P041 seemed to have produced an abnormally strong response. It was reported that the post in test 91P041 had a significantly higher weight than the other posts that were tested.

First, a failure pressure was sought that would produce a response resembling the three similar pendulum tests. The upper graph in Figure 3 shows the response of the BCT model in simulation with a failure pressure of -90 MPa. Many similarities can be seen from the comparison between acceleration plots; the events have approximately the same duration and the initial peak accelerations are in the seven to eight g's range. For statistical comparison, Test 91P039 acceleration data was compared to the simulation data. The total energy dissipated in the simulated event was 94 percent of the energy dissipated in the actual

pendulum test. An analysis of the variance shows that the average residual difference between the two curves is 0.19 g's (2.3 percent of the peak test acceleration) and the standard deviation of the residuals is 0.80 g's (9.7 percent of the peak test acceleration). A t-test of 2.13 for the acceleration data lies within the 90 percent confidence t-test of 2.81 indicating that the two curves represent the same event.

Next, a failure pressure was sought that would produce a response similar to that of Test 91P043, the mid-strength pendulum tested post. The lower graph in Figure 3 shows the response of the simulation with a post possessing a failure pressure of -100 MPa. Again, many similarities can be seen from the comparison between acceleration plots. For statistical comparison, Test 91P043 acceleration data was compared to the simulation data. The total energy dissipated in the simulated event was 92 percent of the energy dissipated in the actual pendulum test. An analysis of the variance shows that the average residual difference between the two curves is 0.37 g's (5.2 percent of the peak test acceleration) and the standard deviation of the residuals is 1.25 g's (17.4 percent of the peak test acceleration). A t-test of 2.67 for the acceleration data lies within the 90 percent confidence t-test of 2.81.

Table 2 gives several characteristics of the pendulum tests as well as the simulated tests. A comparison of these results along with the comparison of acceleration histories supports the conclusion that the finite element model of the post is realistic and can be used with confidence in an extensive model of a guardrail terminal system.

POST - SOIL INTERACTION MODELING

The lateral stiffness of the posts in a guardrail system arises from the posts being driven into the soil. The post-soil interaction may be analyzed by considering the post to be laterally loaded piles. There are numerous modeling techniques for solving laterally loaded pile problems, although, such techniques generally have been for static conditions. In finite element analysis of such cases there are two basic approaches that are commonly employed: 1) the finite element approach in which the post is embedded in a soil continuum of

solid finite elements and 2) the subgrade reaction approach in which the post is supported by an array of uncoupled springs.

Some researchers have made efforts to model the post-soil interaction using the finite element approach. In this approach, finite element models are constructed of the posts embedded in a continuum of soil using three-dimensional solid elements. Although explicit modeling of the posts, the soil, and the interface between the two is conceivably the most formidable method of modeling this intricacy, it may not be the most efficient or practical for routine analysis due to the immense computational demand. It appears that the subgrade reaction approach, in which the posts are supported by an array of uncoupled springs, is the most versatile and practical method of analyzing the post-soil interaction.

Subgrade Reaction Approach

The horizontal subgrade modulus of the soil, which is used in defining the stiffness of the nonlinear springs, is fundamental in determining the soil-resistance of the posts. However, there is no standard value for the horizontal subgrade modulus and the literature provides a wide range of possible values.(11) The horizontal subgrade modulus k_h is given by the relationship:

$$k_h = \frac{F}{A * y} \quad (1)$$

where F is the horizontal reaction force, A is the area over which the force is applied and y is the resulting displacement.

The subgrade modulus is influenced by many factors such as the relative density and moisture content of the soil, the cohesiveness of the soil, the overburden pressure, the nature of the applied load, the post deflection, and the properties and geometry of the post.(11) The value of the subgrade modulus is usually obtained by means of various empirical relationships that have been presented in the literature.(4)(11)

The method used in this study was the one proposed by Habibagahi and Langer which is based upon

the bearing capacity concept.(11) The soil is assumed to be a granular, non-cohesive soil and k_h is a function of deflection y and the effective overburden stress, σ_e , defined by:

$$k_h = N_q \frac{\sigma_e}{y} \quad (2)$$

In which N_q is a lateral bearing capacity factor dependant upon deflection, y , as well as depth, Z , and post width, B . N_q is obtained from the relationship:

$$N_q = A + \sqrt{Z/B} \quad (3)$$

The unitless parameter A , defined below in equation 4, is obtained empirically from load curve data and is dependent upon the angle of internal friction of the soil, ϕ , and the post deflection. In this study the load curve data presented in Habibagahi et al.(11) for a soil with a value of $\phi = 30^\circ$ was used to determine A . In order to incorporate the value of A into the equation above, the method of least squares was employed to obtain a Prony series curve fit from the test data. The equation for A is given below with one deflection dependent term. A comparison of the curve fit and test data is shown in Figure 4.

$$A = 15.276 - 14.09e^{-0.1245y} \quad (4)$$

For a given soil type and gradation, the density and the water content are perhaps the most significant parameters affecting soil strength. The effective overburden pressure, σ_e , used in equation 2, is a function of soil density and water content. As the density of the soil increases, the overburden pressure increases, thereby, increasing soil strength. Soil strength also increases as the moisture content increases, until the soil approaches saturation.(12)(13) At the point of saturation the effective overburden pressure becomes the total applied stress minus the pore water pressure, which consequently reduces the strength of the soil.

The angle of internal friction is also affected by soil type and density, but it is only slightly affected

by water content. Values of ϕ , for various soil types and densities, may be obtained from charts and tables that are available in the literature. (14) (15) The charts and tables commonly present a range of ϕ values for a given soil type that correspond to various particle gradation, soil compaction and relative densities of the soil. Values of ϕ typically range from 30° to 35° for poorly graded sands to as high as 45° to 50° for dense granular soils. The presence of moisture in granular or sandy soils results in only a 1° to 2° decrease in the value of ϕ than if the soils were dry. (16)

The value of k_n given by Equation 1 yields values which approach those obtained by Terazaghi's method and the Navy Design Manual when the deflections are slightly in excess of one inch and the embedment depth is less than 1000 mm, as is the case for guardrail posts. Since there was no load curve data available to develop a direct relationship between the value of A , used in Equations 3 and 4, and ϕ , the relationship was projected into the equations in the form of a modification factor. This factor is based upon a comparison of subgrade modulus values given by the Navy Design Manual for an embedment depth of 500 mm and a lateral post deflection of 34 mm. According to the Navy Design Manual and Terazaghi's method, the subgrade modulus values tend to increase linearly with ϕ when ϕ is in the range from 30° to 42° . The modification factor, MF, is a function of ϕ and is given by:

$$MF = \frac{2}{3}(\phi - 30) + 1 \quad (5)$$

To develop more accurate relationships between A and ϕ for guardrail posts embedded in various strength soils an extensive testing program is needed.

Finite Element Model

A finite element model of a 150x200 mm strong-post was developed and used in the post-soil interaction simulation. The strong-post that is modeled in the simulation is 1,848 mm long with 1,118 mm of the post embedded in the soil. To model the soil's interaction with the post, springs were placed along the faces of

the post on two adjacent sides beginning at the first element nodes below grade and extending to the bottom of the post, as shown in Figure 5. (For sake of simplicity all of the springs were not shown in the figure.) The stiffness of the springs is provided by load curves defined by Equation 1 in which the spring stiffness increases with depth.

The strong-post-soil model consists of 1,332 solid hexahedron elements and 154 discrete nonlinear springs. The volume integration of the solid elements is carried out using one-point Gauss quadrature and the hourglassing modes are controlled by using the Flanagan-Belyschko stiffness form of hourglass control. The post material properties are modeled as isotropic elastic-plastic (material type 3 in LS-DYNA3D) with no failure criteria since the objective is to isolate the soil properties. Table 1 shows the properties of the material model used in the post.

Often times in the analysis of laterally loaded posts, the posts are supported in the vertical direction at the point of rotation. To place a constraint on the posts at such a location is not appropriate for the post-soil model subjected to large deflections because this point will actually tend to move upward as the post is being pushed over. The most practical location for the constraint would be at grade level.(17) Even though some vertical displacement is expected at grade level as that portion of the post pushes down onto the soil, the amount of deflection is minimal and its effect on the simulation was considered to be insignificant. The post was therefore constrained at one node in the vertical direction at grade level.

Pendulum Test Comparison

To validate the model's fidelity, comparisons were made to pendulum test data obtained from a study performed by Holloway et al.(13) The purpose of their research was to develop guardrail post models using the BARRIER VII computer code, and to determine the input parameters for the code corresponding to the various conditions a post may encounter as part of a guardrail system. In their study a number of pendulum tests were performed at Midwest Roadside Safety Facility. The tests involved steel and timber strong-posts

embedded in two types of soils: cohesive and noncohesive. The noncohesive soil was a fine poorly graded sand classified as an A-3 soil under the AASHTO soil classification system. The pendulum tests with the posts embedded in noncohesive soil were performed in unsaturated conditions. Neither the compaction nor the relative density of the noncohesive soil type was given in the report, although, these parameters were reported for the cohesive soil types. The timber posts were rough sawed 150x200 mm Southern Yellow Pine.(13)

The vehicle used in the pendulum tests was the MwRSF bogie which is a rigid steel frame cart. The bogie was ballasted to a test mass of 1,388 kg and the impact speed was 9,144 mm/second. The bogie head was an eight-inch concrete filled standard steel pipe mounted 533 mm above grade.(13) The advantage of using data from rigid bogie tests as a means of validating the post-soil model is that the measured energy dissipated during the impact is directly related to the energy dissipated in the post and the soil, and not to the crushing of the bogie vehicle. A finite element model of the bogie head was developed and was modeled as a rigid body in LS-DYNA3D. The model of the bogie and the post is shown in Figure 5.

A comparison was made between the tests and the simulation using various values for ϕ to define the stiffness of the springs in the model. The bogie impacts the post at 534 mm above grade at a velocity of 9,144 mm/second. The dry unit weight of the test soil was not reported, therefore an estimated value of $1.806\text{E-}05 \text{ N/mm}^3$ (115 lbs/ft^3) was used in the calculations. A value for ϕ of 35° in the simulation yielded results that compared well to the results obtained from test data, as shown in Figure 6.(13) The initial impact forces are much higher in the simulation than in the test due to the high contact stresses produced when the rigid bogie contacts the deformable post, but over the duration of the impact event the simulated response correlates well with the test data.

The soil used in the test was regarded as a weak soil which corresponds to the low value of ϕ used in the simulation. There are many cases however, where the posts are embedded in a well-graded stiff soil with a dry unit weight greater than $2.04\text{E-}05 \text{ N/mm}^3$ and values of ϕ near 45° , in which case the force levels

will be much higher.(4)

In Holloway's tests it was reported that the posts rotated about a point 762 mm below grade. In the simulation the post began to rotate at approximately 812 mm below grade which compares relatively well with the results of tests reported in the literature.(13)(4) For large displacements the rotation point changes as the post continues to rotate and push out of the ground. This event is often neglected in most post-soil models, however, choosing grade level as the location for the post constraint the simulated post's rotation reflects those observed in pendulum tests. Figure 7 shows the post rotation as a result of the finite element simulation.

CONCLUSIONS

The foregoing sections have discussed the finite element modeling of wooden guardrail posts and the posts' interaction with the soil during impact events using the nonlinear finite element program LS-DYNA3D. The posts, the soil, and their interaction are fundamental components of a guardrail system that have considerable influence upon the response of the system. These components must be modeled accurately in order to obtain valid results from impact simulations.

A finite element model of a wood BCT post was developed and compared to pendulum test data. The material model used for the post was an isotropic elastic-plastic model which sufficiently simulated the failure mode observed in wooden guardrail posts during impact. A statistical analysis was performed to validate the results of the model and it was concluded that the finite element model is realistic and can be used with confidence in an extensive model of a guardrail system.

The post-soil interaction was modeled using the subgrade reaction approach which involves an array of nonlinear springs attached along the length of the post below grade. This modeling technique was compared to pendulum test data of a strong-post embedded in a fine poorly graded sand and the simulated results correspond well to the test data.

REFERENCES

1. M H Ray and G S Patzner, 'A Finite Element Model of the Modified Eccentric Loader Breakaway Cable Terminal (MELT)', Transportation Research Paper No. 970367, Transportation Research Board, Washington D.C., 1997.
2. J R Rohde, B T Rosson, and R Smith, 'Instrumentation for Determination of Guardrail-Soil Interaction', Transportation Research Report No. 1528, Transportation Research Board, Washington D. C., 1996.
3. D Stout, J Hinch and T L Yang, 'Force Deflection Characteristics of Guardrail Posts', FHWA Report No. FHWA-88-193, Federal Highway Administration, Washington D.C., September 1988.
4. J F Dewey, J K Jeyapalan, T J Hirsch and H E Ross, 'A study of the Soil-Structure Interaction Behavior of Highway Guardrail Posts', FHWA/TX-84/12+343-1, Texas Transportation Institute, July 1983.
5. G S Patzner, C A Plaxico, and M H Ray, 'Effects of Wood Post and Soil Strength on the Performance of the Modified Eccentric Loader Breakaway Cable Terminal (MELT) in an NCHRP Report 350, Test 3-35 impact scenario', unpublished draft, 1997.
6. Wood Handbook : Wood as an Engineering Material, United States Department of Agriculture, U.S. Government Printing Office, Washington, D.C., 1987.
7. CM Brown, 'Pendulum Testing of BCT Wood Posts, FOIL Tests: 91P039 through 91P045', Federal Outdoor Impact Laboratory (FOIL), McLean, Virginia, August 1991.
8. J O Hallquist, *LS-DYNA3D Theoretical Manual*, LSTC Report 1018 Revision 3, Livermore Software Technology Corporation, April 1994.
9. J O Hallquist, D W Stillman and T L Lin, *LS-DYNA3D Users Manual-Version 930, 'A Nonlinear, Explicit, Three-Dimensional Finite Element Code for Solid and Structural Mechanics'*, Livermore Software Technology Corporation, April 1994.
10. R D Cook, Finite Element Modeling for Stress Analysis, John Wiley & Sons, Inc., 1995.

11. K Habibagahi and J A Langer, 'Horizontal Subgrade Modulus of Granular Soils', in Laterally Loaded Deep Foundations, Langer, Mosely and Thompson, eds.,ASTM Publication Code No. 04-835000-38, American Society for Testing Materials, 1984, pp.21-34.
12. J D Michie, M H Ray, W W Hunter and J Stutts, 'Evaluation of Design Analysis Procedures and Acceptance Criteria for Roadside Hardware,' Contract No. DTFH61-82-C-00086, Southwest Research Institute, October 1985.
13. J C Holloway, M G Bierman, B G Pfeifer, B T Rossen and D L Sicking, 'Performance Evaluation of KDOT W-Beam Systems Volume II: Component Testing and Computer Simulation', Report No. TRP-03-39-96, Midwest States Regional Pooled Fund, May 1996.
14. J E Bowles, Foundation Analysis and Design, Fourth Edition, McGraw-Hill Publishing Company, 1988.
15. I S Dunn, L R Anderson and F W Kiefer, Fundamentals of Geotechnical Analysis, John Wiley & Sons, New York, 1980.
16. R D Holtz, An Introduction to Geotechnical Engineering, Prentice-Hall, Englewood Cliffs, New Jersey, 1981.
17. R L Sogge, 'Microcomputer Analysis of Laterally Loaded Piles,' in Laterally Loaded Deep Foundations: Analysis and Performance, ASTM STP 835, J A Langer, E T Mosely and C D Thompson, Eds., American Society for Testing and Materials, 1984, pp. 35-48.

Table 1. Timber material properties

Non-failing region:		
Material type	3	Isotropic-elastic-plastic
Element type	solid	1-point integration
Density	610	kg/m ³
Mod. of elasticity	11	GPa
Poisson's ration	0.3	
Yield stress	40	MPa
Tanget modulus	11	MPa
Failure region:		
Material Type	13	Isotropic-elastic-plastic with failure
Element type	solid	14-point integration
Density	610	kg/m ³
Poisson's ration	0.3	
Shear Modulus	4231	MPa
Bulk Modulus	9167	MPa
Yield Stress	40	MPa
Failure pressure	-90	MPa

Table 2. Pendulum test and simulation results

Test Number	Impact Speed (m/s)	Change in Velocity (m/s)	Peak Acceleration (g's)	Honeycomb Crush (mm)
91P039	8.90	0.819	-7.22	152
91P040	8.99	0.850	-7.18	160
91P041	9.08	2.87	-8.99	320
91P042	8.93	0.746	-6.59	163
91P043	8.93	1.30	-7.22	206
Simulation (fp=-90)	8.90	0.744	-7.16	152
Simulation (fp=-100)	8.90	1.15	-7.68	197

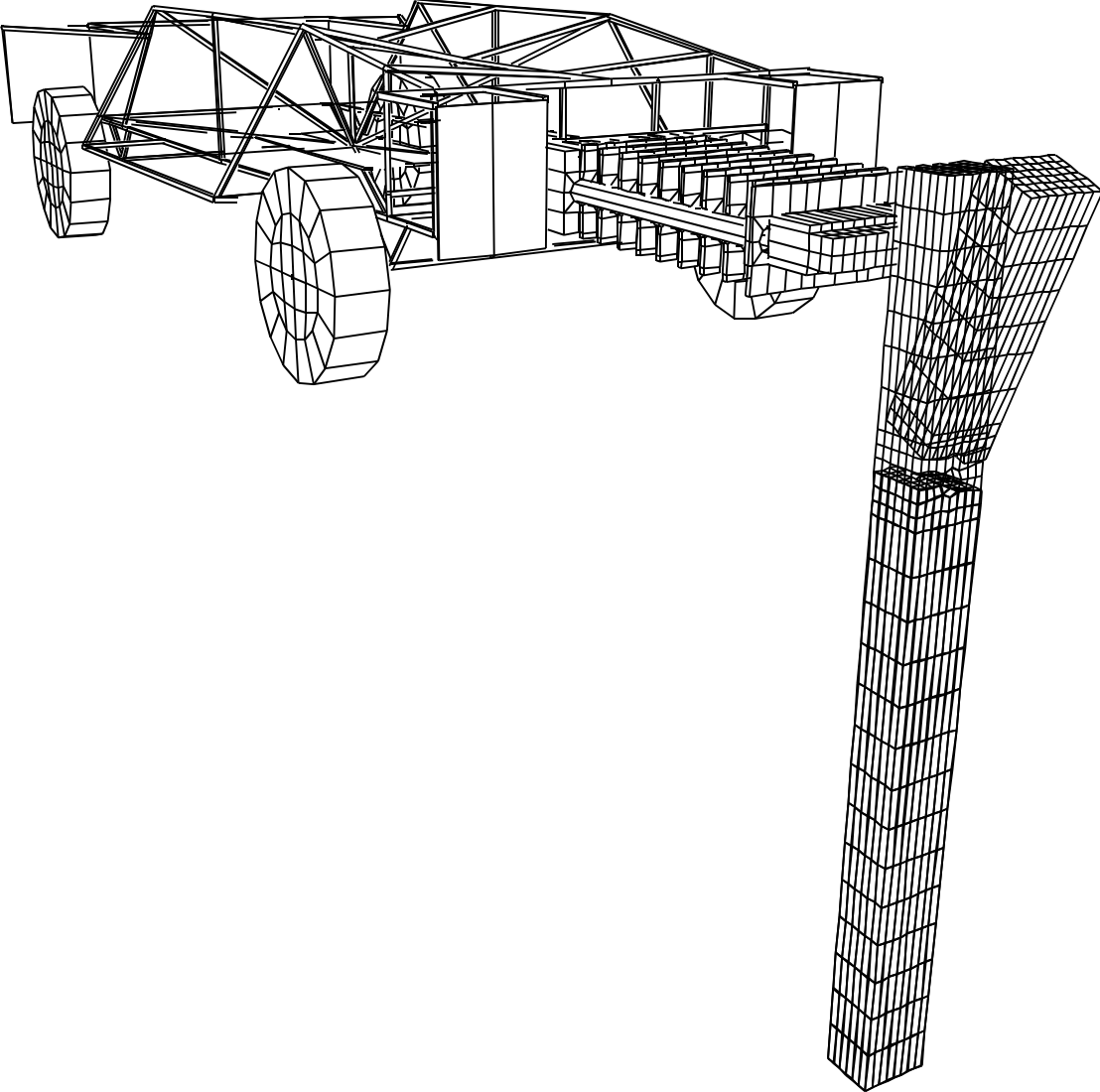


Figure 1. BCT post - NCAC bogie configuration

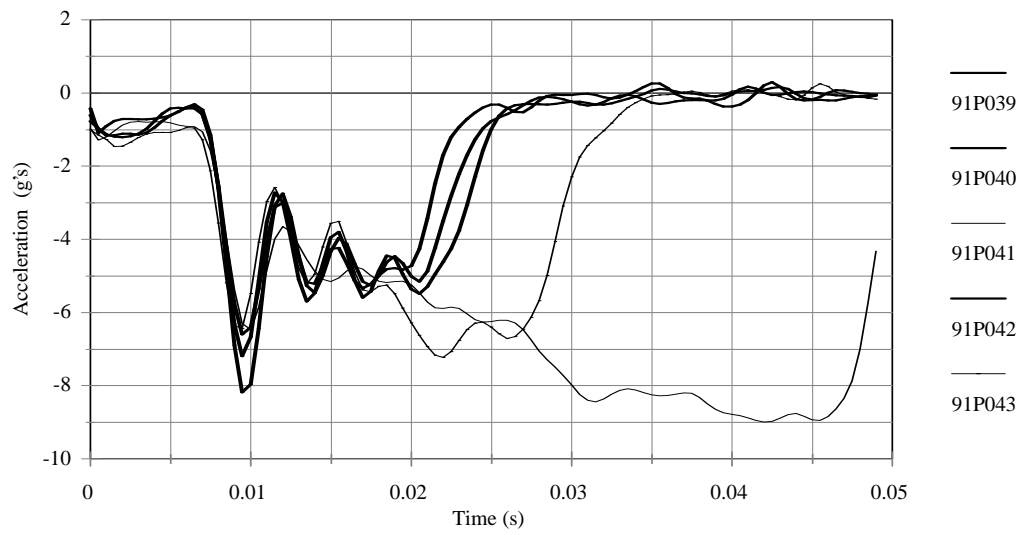


Figure 2. BCT post pendulum test acceleration histories

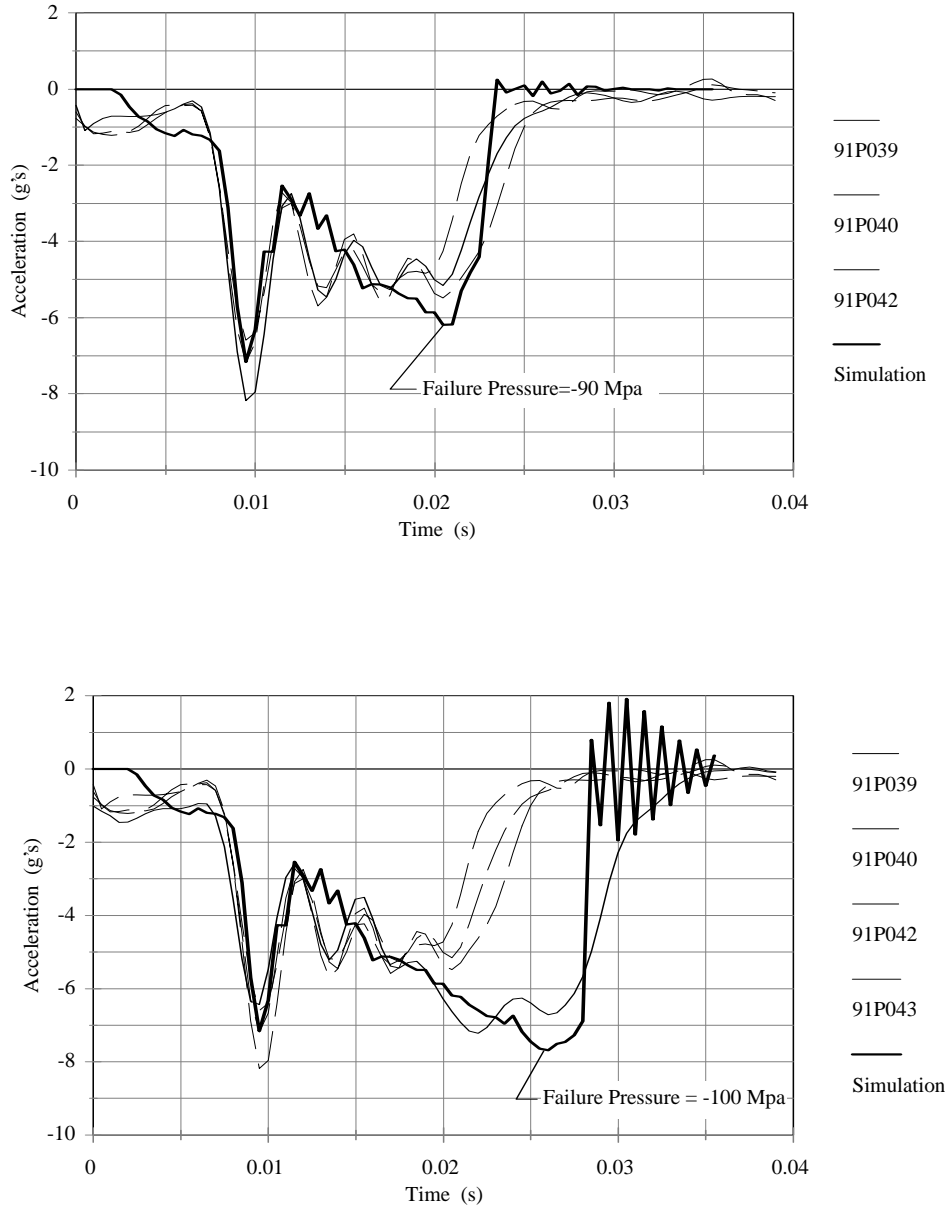


Figure 3. Comparison of BCT post pendulum tests and simulation

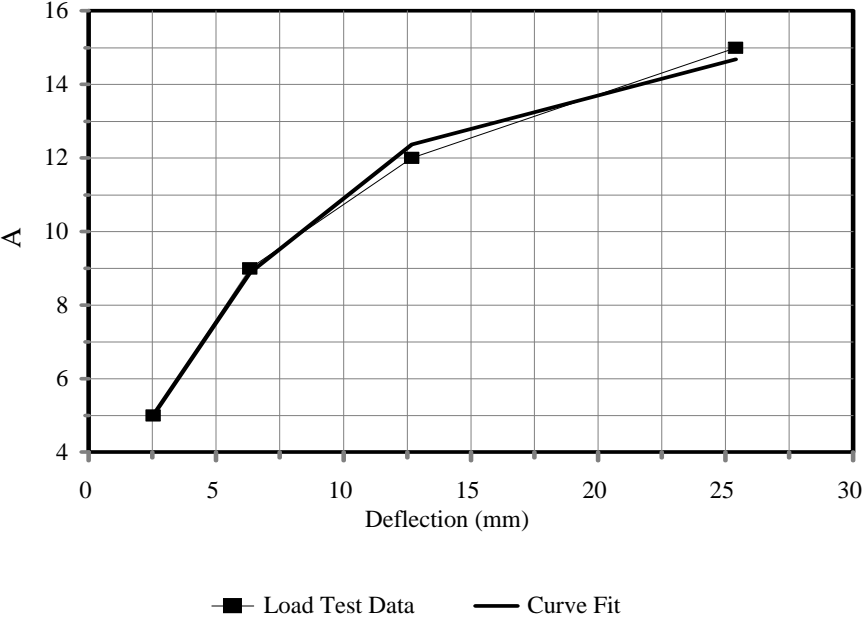


Figure 4. A vs. deflection (mm) for load test data at $\phi = 30^\circ$

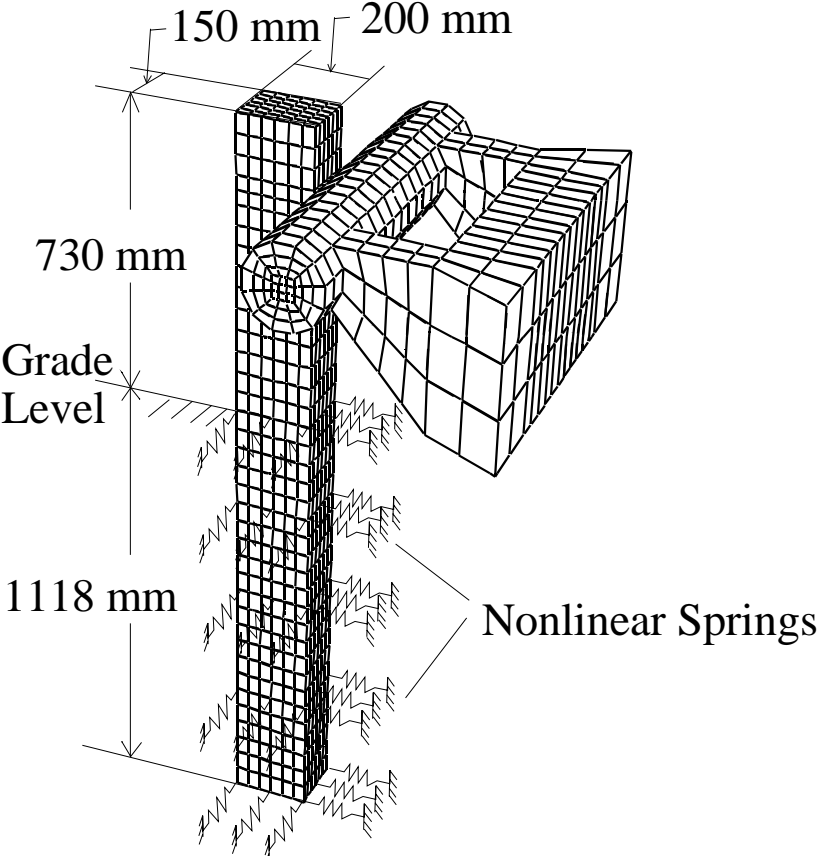


Figure 5. Finite element model of strong-post and MwRSF bogie head

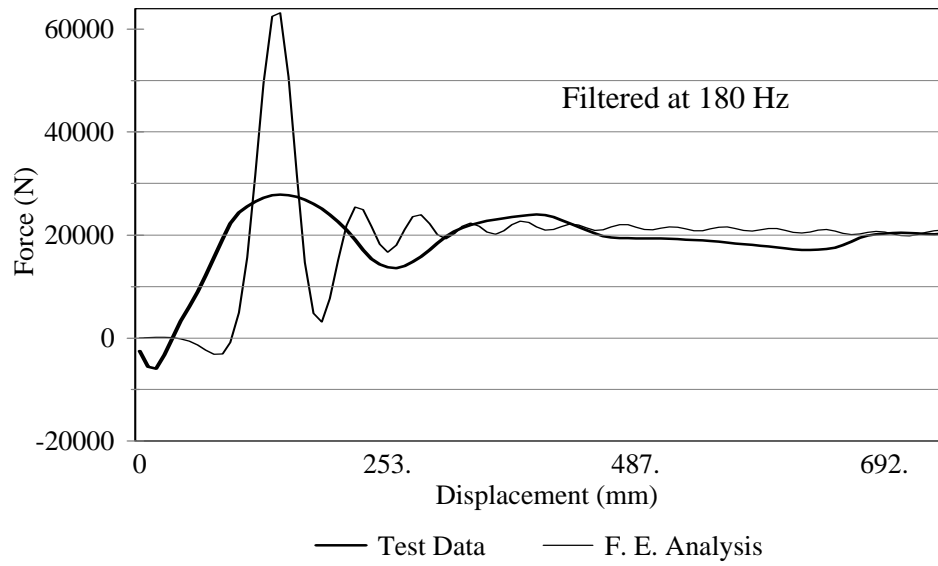


Figure 6. Force vs deflection of pendulum test and finite element simulation

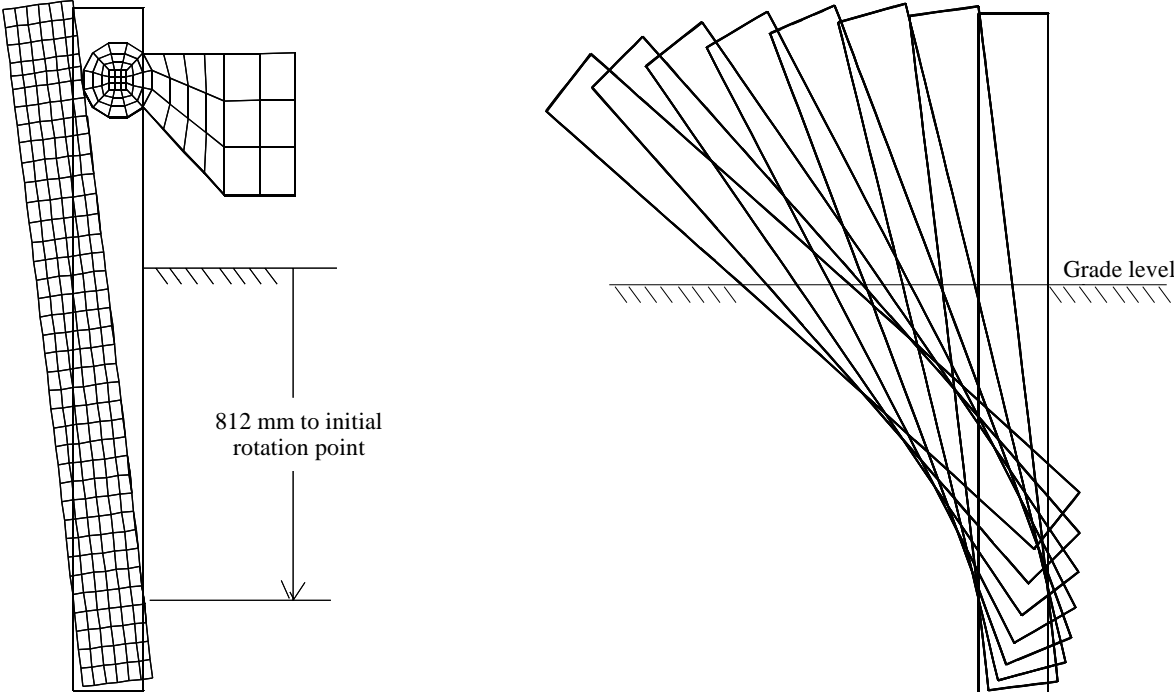


Figure 7. Simulated response of MwRSF bogie impacting a strong-post embedded in weak soil